Variability of North Atlantic heat transfer during MIS 2

M. Weinelt,[1] E. Vogelsang,[1] M. Kucera,[2] U. Pflaumann,[1] M. Sarnthein,[1] A. Voelker,[1] H. Erlenkeuser,[3] and B. A. Malmgren[4]

Received 11 February 2002; revised 14 January 2003; accepted 24 February 2003; published 30 August 2003.

[1] Short-term changes in sea surface conditions controlling the thermohaline circulation in the northern North Atlantic are expected to be especially efficient in perturbing global climate stability. Here we assess past variability of sea surface temperature (SST) in the northeast Atlantic and Norwegian Sea during Marine Isotope Stage (MIS) 2 and, in particular, during the Last Glacial Maximum (LGM). Five high-resolution SST records were established on a meridional transect (53°N–72°N) to trace centennial-scale oscillations in SST and sea-ice cover. We used three independent computational techniques (SIMMAX modern analogue technique, Artificial Neural Networks (ANN), and Revised Analog Method (RAM)) to reconstruct SST from planktonic foraminifer census counts. SIMMAX and ANN reproduced short-term SST oscillations of similar magnitude and absolute levels, while RAM, owing to a restrictive analog selection, appears less suitable for reconstructing "cold end" SST. The SIMMAX and ANN SST reconstructions support the existence of a weak paleo-Norwegian Current during Dansgaard-Oeschger (DO) interstadials number 4, 3, 2, and 1. During the LGM, two warm incursions of 7°C water to occurred in the northern North Atlantic but ended north of the Iceland Faroe Ridge. A rough numerical estimate shows that the near-surface poleward heat transfer from 53° across the Iceland-Faroe Ridge up to to 72° N dropped to less than 60% of the modern value during DO interstadials and to almost zero during DO stadials. Summer sea ice was generally confined to the area north of 70°N and only rarely expanded southward along the margins of continental ice sheets. Internal LGM variability of North Atlantic (>40°N) SST in the GLAMAP 2000 compilation [*Sarnthein et al.*, 2003b; *Pflaumann et al.*, 2003] indicates maximum instability in the glacial subpolar gyre and at the Iberian Margin, while in the Nordic Seas, SST was continuously low. *INDEX TERMS:* 1833 Hydrology: Hydroclimatology; 3344 Meteorology and Atmospheric Dynamics: Paleoclimatology; 4267 Oceanography: General: Paleoceanography

Citation: Weinelt, M., E. Vogelsang, M. Kucera, U. Pflaumann, M. Sarnthein, A. Voelker, H. Erlenkeuser, and B. A. Malmgren, Variability of North Atlantic heat transfer during MIS 2, *Paleoceanography*, *18*(3), 1071, doi:10.1029/2002PA000772, 2003.

1. Introduction

[2] The Last Glacial Maximum (LGM), defined by maximum ice sheet extension [*Teller*, 1987], is generally considered a fairly stable climatic phase with minimum heat transport to the high northern latitudes, as a result of a weakened Atlantic thermohaline circulation (THC) [e.g., *Broecker*, 1997]. Past sea surface temperature (SST) reconstructions of the LGM Atlantic [*CLIMAP Project Members*, 1976, 1981] indicate an equilibrium state decidedly different from that of today and have been employed as boundary conditions to initiate and validate numerical climate models (e.g., PMIP Project; *Joussaume and Taylor* [1995]; *Kutzbach et al.* [1993]).

[3] The growth of the modern coretop data base over the last 20 years and improved computational techniques to derive paleotemperatures [*Pflaumann et al.*, 1996; *Waelbroeck et al.*, 1998; *Malmgren et al.*, 2001] from census counts of planktonic foraminifera have encouraged new reconstructions of glacial SST [e.g., *Mix et al.*, 1999; *Pflaumann et al.*, 2003]. Simultaneously, the development of a high-resolution (centennial to decadal) timescale, and a growing array of high-resolution sediment records, have improved the temporal definition of the LGM interval and enabled a better comparison of climate archives in ocean sediments and ice cores (summary of *Mix et al.* [2001]).

[4] Various strategies have been employed to define the time interval best representing the LGM. The EPILOG working group [*Mix et al.*, 2001] defined the LGM through the insolation minimum at 21,000 ± 2000 years BP (in this article, all dates are cited as calendar years) and the last maximum sea level lowstand which lasted from 23,000 until 19,000 years BP, where a first deglacial sea level rise of 15 m is inferred [*Yokoyama et al.*, 2000]. Since the older portion of the lowstand is based on few data, GLAMAP 2000 (Glacial Atlantic Mapping 2000; *Sarnthein et al.* [2003a]) defined the duration of a climatically stable LGM by the Last $\delta^{18}O$ Isotopic Maximum (LIM) in marine Atlantic records, which lasted from 21,500 until 18,000

[1]Institut für Geowissenschaften, Kiel University, Kiel, Germany.
[2]Department of Geology, Royal Holloway College, University of London, Egham, Surrey, UK.
[3]Leibniz Labor für Altersbestimmung und Isotopenforschung, Kiel University, Kiel, Germany.
[4]Department of Earth Sciences-Marine Geology, Göteborg University, Göteborg, Sweden.

0883-8305/03/2002PA000772

years BP (17,500 years BP, according to N. J. Shackleton (personal communication 2000)), that is until immediately prior to the onset of major deglaciation. Prior to 22,500–22,000 years BP (on the GISP2 timescale; *Stuiver and Grootes* [2000]), North Atlantic surface water records are expected to show considerable instability linked to Heinrich Event 2 and the subsequent Dansgaard-Oeschger (DO) interstadial 2. Therefore GLAMAP 2000 decided to exclude this interval from their LGM SST compilations of the North Atlantic [*Pflaumann et al.*, 2003].

[5] Any reconstruction of Atlantic LGM SST must also address the question of the internal stability of this 3500-year interval. Conditions in the high-latitude North Atlantic are important in controlling the strength and configuration of Atlantic THC. Short-term changes in factors controlling the surface water density and convection may be highly efficient in disturbing the ocean ''conveyor'' system on short timescales, thus affecting global climate stability. Meltwater injections from the ambient ice sheets are likely candidates for triggering, or at least amplifying, short-term perturbations of the THC, as was shown for DO cycles during marine isotope (MIS) stage 3 and early MIS 2 [*Van Kreveld et al.*, 2000]. However, during late MIS 2, the continuation of such cycles appears less evident [e.g., *Blunier et al.*, 1998]. Both the GRIP and GISP2 ice records [*Johnson et al.*, 1992; *Grootes and Stuiver*, 1997; *Stuiver and Grootes*, 2000] indicate that abrupt, short-term atmospheric warmings and coolings over Greenland were suppressed between 23,000 and 18,000 years BP. The causes for this quiet phase remain unclear [*Schulz et al.*, 1999].

[6] In a numerical model, *Charles et al.* [1994] studied the contribution of the Nordic Seas as a vapor source for Greenland precipitation. In the case where it was ice covered sensu *CLIMAP Project Members* [1981], they found that vapor production was halved during the LGM, whereas the contribution of vapor from the midlatitude North Atlantic may have increased by 50%. In contrast, recent SST reconstructions support the conclusion that LGM surface waters in the Nordic Seas remained largely ice-free during glacial summer, allowing a direct heat and moisture transfer between surface water of the northern North Atlantic and the ambient continents [*Hebbeln et al.*, 1994; *Weinelt et al.*, 1996; *De Vernal et al.*, 2000; *Sarnthein et al.*, 2003b; *Pflaumann et al.*, 2003]. In general, short-term variations in northern high-latitude sea-ice cover are still a major unknown amongst climate variables. For example, it remains unclear whether seasonally ice-free surface water in the Nordic Seas is a valid reconstruction for the entire LGM interval, or was just a rare extreme.

[7] Assessing the centennial-scale variability of glacial surface conditions in the northern North Atlantic may therefore provide a key to a better understanding of glacial boundary conditions. Moreover, new high-resolution data may lead to a better understanding of processes that control the onset and end of the LGM, producing scenarios that can be tested in future climate models.

[8] To address these questions, this study aims: (1) to establish a precise chronology of short-term SST fluctuations in the middle- to high-latitude North Atlantic during MIS 2, revealing their amplitudes, timing, and duration, and to compare the amplitudes of SST variability related to DO cycles and the internal variability within the subsequent LGM interval; (2) to identify the North Atlantic regions which underwent major SST variability within the LGM; and finally, (3) to outline patterns of maximum and minimum sea-ice distribution.

2. Methods and Strategy

[9] A transect of five SST records (Figure 1) was established using sites below the track of the modern North Atlantic Drift (Kiel core 23415 at 53°N, 19°W), at the southern slope of the Iceland-Faroe Ridge (IFR; a composite record of Kiel cores 16396 and 16397, 62°N, 11°W), and beneath the Norwegian Current from the Vøring Plateau and the Bear Island Fan (Kiel cores 23071 and 23074, 67°N, 3° and 5°E; core MD95-2012, 72°N, 11°E). This meridional transect was employed to document changes in the heat transport to high latitudes during MIS 2.

2.1. $\delta^{18}O$ and Ice Rafted Detritus (IRD) Records

[10] To identify meltwater fluxes related to iceberg melt, $\delta^{18}O$ records of *N. pachyderma* sin. and IRD counts were used. IRD grains were counted in the size fraction >150 μm and are given as percentage of the total coarse fraction. $\delta^{18}O$ was measured on at least 25 specimens of *N. pachyderma* sin. (150–250 μm). The tests were treated with 99.8% ethanol, cracked, and ultrasonically cleaned for 30 s. $\delta^{18}O$ measurements were performed at the Leibniz Laboratory of Kiel University using a Finnigan MAT-251 coupled to an automated Carbo-Kiel preparation line. Analytical precision of $\delta^{18}O$ measurements was 0.07‰. The $\delta^{18}O$ and IRD records of core MD 95-2012 are from *Dreger* [1999]; the $\delta^{18}O$ records of cores 23074 and 23071 are from *Voelker* [1999].

2.2. Chronology

[11] Age models are based on 38 Accelarator Mass Spectrometry (AMS) ^{4}C dates on monospecific samples of *Neogloboquadrina pachyderma* sin. (corrected for 400-year reservoir age) which were converted to calendar ages (back to 24 cal ka using INTCAL 98 [*Stuiver et al.*, 1998]; beyond 24 cal ka using *Voelker et al.* [1998, 2000]) (Table 1; Figure 2). In addition, we employed GISP2 ages, which are based on annual-layer counting with an error range of ±2% [*Meese et al.*, 1997], for tuning the top and bottom ages of Heinrich layers and those of DO peak interstadials [*Sarnthein et al.*, 2001]. These ages, directly deduced from tuning, yield control points not affected by the potential error linked to fluctuations in the ^{14}C reservoir age, which may reach up to 2000 years during times of high meltwater flux [*Sarnthein et al.*, 2001]. At site 23415, Heinrich (H) layers were directly identified by IRD maxima, paralleled by strongly depleted planktonic $\delta^{18}O$ values resulting from pronounced meltwater anomalies.

[12] At the Iceland-Faroe Ridge and even more so in the Norwegian Sea, high IRD contents in glacial sediments are the rule rather than the exception. Accordingly, Heinrich layers cannot be traced unambiguously at these sites [*Dowdeswell et al.*, 1999; *Fronval et al.*, 1995]. This

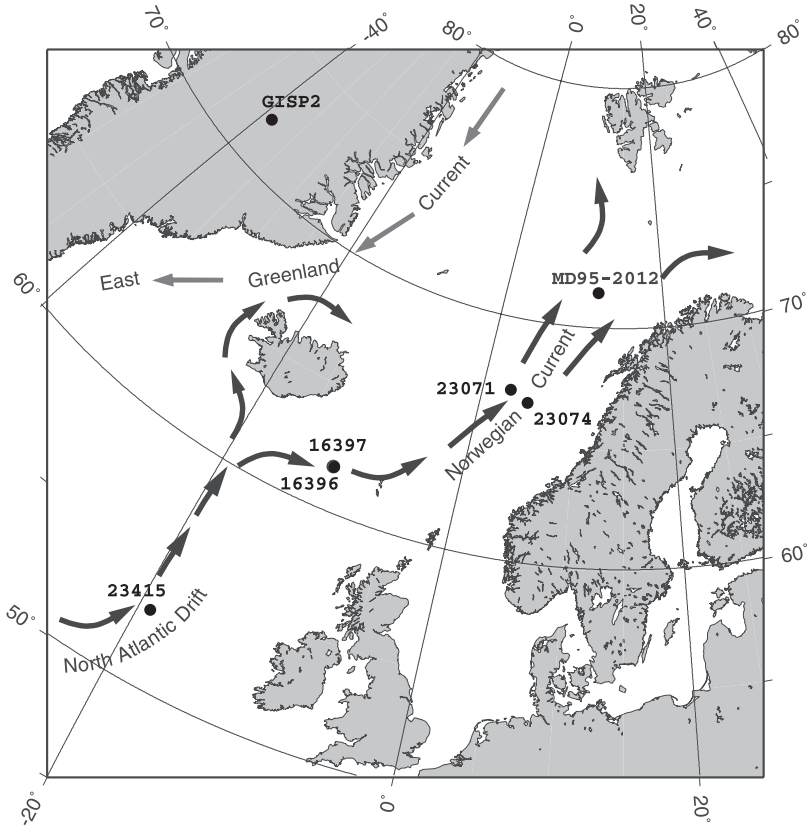

Figure 1. Modern surface currents in the middle- to high-latitude North Atlantic with locations of cores 23415, 16396/16397, 23071, 23074, MD 95-2012, and the GISP2-ice cores 23415, 16396/16397, 23071, 23074, MD 95-2012, and the GISP2-ice core.

holds especially true for H2, where ^{14}C dates in part show a broad scatter [*Dreger*, 1999; *Voelker*, 1999]. In cores 16396/97 and 23074, well-dated $\delta^{18}O$ meltwater excursions, which parallel an IRD maximum and precede a distinct SST maximum, identified as DO interstadial 2, were ascribed to H2. Additional local meltwater spikes occur near 25,000 and 18,500 years B. P. In core 23071 the position of H2 can only be identified by subsequent, fairly well dated minor temperature spikes interpreted as DO interstadial 2. Here a minor $\delta^{18}O$ meltwater signal occurs subsequent to this interstadial (Figure 2c). The age model of core MD95 2012 (Figure 2e) is based entirely on tuning the variations in magnetic susceptibility to the magnetic susceptibility record of the well dated core MD 95 2010 from the Vøring Plateau, which displays a highly similar curve structure (M. Pirrung, personal communication, 2001; M. Pirrung, manuscript in preparation, 2003). For core MD 95 2010, *Dokken and Jansen* [1999] found a close correlation of maxima in magnetic susceptibility (in the Norwegian Sea related to IRD minima) with the DO interstadials in the GISP2 record.

[13] The five cores show medium to high sedimentation rates ranging from 4 to 263 cm/kyr (Table 1). Thus a temporal resolution of 100 to 300 years can be achieved by sampling at intervals of 1 to 2 cm, sufficient to depict oscillations in the range of Dansgaard-Oeschger interstadials of more than 300 years duration [*Dansgaard et al.*, 1993; *Blunier et al.*, 1998].

2.3. Reconstruction of SST

[14] Previous studies have shown that all census-based SST reconstruction techniques tend to overestimate temperatures at the "cold end" (<3–4°C for summer SST). This means that the magnitude of fluctuations in fossil SST records may be truncated, particularly in polar waters dominated by *Neogloboquadrina pachyderma* sin. (abundance >97%) [*Pflaumann et al.*, 1996; *Weinelt et al.*, 1996, 2001; *Malmgren et al.*, 2001]. In other regions, the techniques seem to underestimate SST in the range of 5–7°C, yielding SST reconstructions as low as 4–5°C. In the modern northern North Atlantic, surface waters in the SST range of 5–7°C are confined to the narrow Arctic front, where warm Atlantic water masses encounter cool water masses of the Arctic Domain, and are therefore only represented by few modern samples [*Pflaumann et al.*, 2003]. In summary, the method-related overestimates and underestimates in the temperature range of 3–7°C may somewhat obscure the real range of SST fluctuations. To minimize this potential bias in our SST reconstructions, the following strategies were employed [see also*Pflaumann et al.*, 2003]):

[15] 1. From 600 to 1400 (a mean of 800) specimens were counted per sample, to better estimate the true proportion of

Table 1. Age Control and Temporal Resolution of Paleoceanographic Records[a]

Depth, cm	HE, DO IS ^{14}C Age ± err,[b] years	Calendar Age, kyr
	Core 16396	
180	13970 ± 80	16.76
198	base H1	18.10
198	15.08 ± 150	(18.00)
290	15.73 ± 100	18.78
430	16830 ± 90	20.04
530	17400 ± 90	20.69
	Core 16397	
10	15550 ± 80	18.60
82	17770 ± 120	21.09
225	top H2	23.40
230	20550 ± 140	24.04
240	base H2	24.20
	Core 23071	
74.5	11760 ± 100	
85	12550 ± 220	
93.5	13835 ± 100	
96	14790 ± 190	
105.5	base H1	18.10
130	16990 ± 220	
160	18790 ± 240	
220	23.73	
257	top H3	29.0
264	26350 ± 340/ base H3	30.20
	Core 23074	
47.5	11920 ±70	13.95
68.5	12420 ± 70	14.35
94.5	13450 ± 70	16.16
112.5	14780 ± 100	(17.69)
124.5	base H1	18.10
135.5	15500 ± 80	18.52
190.5	15980 ± 110	19.07
230.5	16580 ± 100	19.76
245.5	16880 ± 110	20.10
304.5	17570 ± 120	20.90
324.5	17980 ± 110	21.37
355.5	18120 ± 130	21.53
377.5	18330 ± 130	21.77
399.5	18830 ± 140	22.3
412.5	19270 ± 150	22.85
422.5	19540 ± 140	23.17
483	top H2	23.40
628.5	DO IS 3	27.80
644.5	DO IS 4	28.80
663.5	top H3	29.00
	Core 23415	
117.5	top H1	14.67
131	base H1	18.10
135	15260 ± 80	1824
145	15810 ± 100	18.87
155	17300 ± 110	20.59
162.5	17780 ± 120	21.26
183	top H2	23.40
195	21310 ± 210	24.20
	base H2	
202.5	22520 ± 180	26.02
210	23270 ± 190	26.77
225	top H3	29.00
233	base H3	30.20
242.5	27500 ± 320	31.00
	Core MD95 2012	
100.5	end of Younger Dryas	11.64
180.5	Bølling	
210.5	12790 ± 70	
262.5	base H1	18.10
618.5	start	23.40
	DO IS 2	
819.5	DO IS 3	27.80
868.5	start	29.00
	DO IS 4	
940.5	29080 ± 390	

Core	Average Sedimentation Rate, cm/kyr	Average Temporal Resolution, years δ^{18}O	SST
16396	118	80	
16397	43 (8–62)	220	280
23071	8 (6–14)	80	170
23074	41 (14–263)	25	135

[a] ^{14}C ages are corrected for reservoir age of −400 years.
[b] HE, Heinrich event; DO IS, Dansgaard Oeschger Insterstadial.

rare subpolar species in the census [*van der Plas and Tobi*, 1965]; e.g., for a species percentage of 4% the relative error is 40–20% at 2σ). In case of specimen numbers smaller than 600, we averaged the census data of two or more successive samples (in core MD 95 2012).

[16] 2. Three different computational techniques were used to derive the SST estimates: Similarity Maximum (SIMMAX; *Pflaumann et al.* [1996, 2003]), Revised Analog Method (RAM; *Waelbroeck et al.* [1998]), and back propagation Artificial Neural Networks (ANN; *Malmgren et al.* [2001]). The simultaneous application of three different computational approaches allows a more robust assessment of the reliability of the specific SST oscillations and of their absolute values [*Hutson*, 1977; *Malmgren et al.*, 2001].

[17] 3. The percentages of *N. pachyderma* sin. are presented for comparison to discriminate potential water mass fluctuations qualitatively. Today, the percentages of *N. pachyderma* sin. in the Nordic Seas allow a rough classification into Atlantic (<95%), Arctic Domain (97–95%), and Polar (>97–99%) water masses [*Pflaumann et al.*, 1996; *Weinelt et al.*, 1996].

2.4. SST Reconstruction Techniques

[18] The SIMMAX SST estimates in this study are based on the SIMMAX 28 data base, which contains 947 modern coretop samples with SST data (for 10 water depth and summer season) compiled from the Levitus database [*Levitus and Boyer*, 1994]. The parameters of the searching and weighing algorithm were the same as described in *Pflaumann et al.* [1996, 2003].

[19] SIMMAX [*Pflaumann et al.*, 1996] is a variant of *Hutson*'s [1980] Modern Analog Technique (MAT), with the added feature of weighting best analogs by their geographical distance from the fossil sample. The distance weighting favors best analog samples that lie closer than 100/200 km to the fossil sample site [*Pflaumann et al.*, 2003]. One may expect a smoothing of the SIMMAX paleotemperature signal during "no-analog" times because of the attenuated impact of more remote analog samples. On the other hand, by emphasizing "local" analogs, the technique avoids inclusion of spurious or biased analogs from distant regions, possibly inhabited by different genetic types

of the traditionally described morphospecies of planktonic foraminifera. Recent molecular genetic studies have shown that such distinct molecular types may indeed have specific environmental preferences [e.g., *Darling et al.*, 2000]. It has been shown that SIMMAX (using 10 modern analogs) works especially well at the cold end [*Pflaumann et al.*, 1996; *Malmgren et al.*, 2001], although this "pro" may be influenced in almost monospecific faunas by the dominance of distance weighting on the SST signal. To evaluate the SST estimates produced by SIMMAX for times prior to the Holocene, we therefore employed several additional independent techniques.

[20] RAM [*Waelbroeck et al.*, 1998], another variant of MAT, is potentially more sensitive to minor SST changes because of a more restrictive selection of modern analogs, in some cases as few as two. In special oceanographic settings, such as along frontal systems, RAM may thus provide better results. *Malmgren et al.* [2001] demonstrated that at the "cold end" of the SST range, RAM (2-D mapping; $\alpha = 0.2$, $\beta = 10$, $\gamma = R = 0.2°C$, where α is a threshold value of the dissimilarity increase rate; β is the maximum number of analogs retained; γ is the grid step in the environmental space; and R is the interpolation radius; *Waelbroeck et al.* [1998]) produced the highest prediction error. Arguably, this could be due to the low value of parameter α. Similarly, in a test of estimated versus measured SST, RAM ($\alpha = 0.1$, $\beta = 10$, $\gamma = 0.25$, $R = 0.3°C$) produced considerable scatter at the cold end (<5°C), but no systematic under-/overestimates [*Weinelt et al.*, 2001]. In our core records the RAM ($\alpha = 0.5$, $\beta = 10$, $\gamma = 0.4$, $R = 0.5°C$) SST reconstruction, which is based on the same data set for calibration as SIMMAX, appears oversensitive to very small changes in the relative percentages of faunal species. For example, SST estimates were found to jump between −1 and 6°C during cold isotope stages (Figures 2c–2e; see also *Weinelt et al.* [2001]).

[21] The Artificial Neural Networks (ANN) technique is a computer-intensive method, which relies on the sole assumption that there is a relationship between the distribution of modern faunas and the physical properties of the environment. It is based on an algorithm that has the ability of autonomous "learning" of a relationship between two groups of numbers. ANNs have the ability to overcome problems of fuzzy and nonlinear relationships between sets of input and output variables. Each trained neural network serves as a unique transfer function, yet at the same time this highly nonlinear and recurrent function is so complicated that it has the ability to simulate a decision algorithm. The utility of this technique for paleotemperature estimates from faunal census data has been explored by *Malmgren and Nordlund* [1997], and a first set of ANN trained on a large faunal database was developed by *Malmgren et al.* [2001]. This database is the 738-sample (plus two new Caribbean coretops) North Atlantic data set of *Pflaumann et al.* [1996] that forms the backbone of our extended 947-sample data base employed for SIMMAX and RAM SST estimates [*Pflaumann et al.*, 2003]. Thus we have also been able to use *Malmgren et al.*'s [2001] trained ANN to reconstruct paleo-SST in our North Atlantic cores. This ANN has been trained to predict SST as the 0–75 m average, which differs from the 947-sample database that was tied to SST at 10 m. In the Nordic Seas, this difference in water depth used for calibration today results in a lowering of measured temperatures by 1°C [*Levitus and Boyer*, 1994]. As shown in the insert graph in Figure 2a, the SST records of Figure 2 only differ by 0.7°C ± 0.5.

[22] Only summer SST estimates are considered in this study, because winter estimates may be more questionable in high latitudes, where the major plankton growth is limited to peak summer month [*Pflaumann et al.*, 1996; *Carstens and Wefer*, 1997; *Simstich*, 1999; *Jensen*, 1998]. To illustrate the spatial patterns of SST variability within the LGM interval the difference range of maximum and minimum SST was mapped using the GLAMAP 2000 data base [*Pflaumann et al.*, 2003]. Here SST records were only considered from cores where the LGM is represented by 3 and more data points.

[23] A conservative estimate of the maximum extension of sea ice during LGM summer was derived from threshold SIMMAX-SST estimates. Our threshold SST level of 2.5°C for summer (July to September) sea ice is derived for the modern sea ice extension with an average concentration of >50% in the Arctic Ocean (1976–1987; *Gloersen et al.* [1992]) and fully considers the overestimation of modern SIMMAX-based SST values in many polar regions [*Sarnthein et al.*, 2003b]. In summary, where SIMMAX SST exceed 2.5°C, no more summer sea ice with concentrations of more than 50% can be expected.

3. Results and Discussion

3.1. Variations in Heat Advection to Northern High Latitudes During MIS2

[24] In the northeast Atlantic and Norwegian Sea (Figure 2), the $\delta^{18}O$ records of all five cores reveal short, pronounced $\delta^{18}O$ minima that were caused by iceberg melting associated with Heinrich events 3, and/or 2 ($\Delta\delta^{18}O$ 0.7–1.5‰) near 30,200–29,000 years and 24,200–23,400 years BP, respectively) [*Bond et al.*, 1993; *Voelker*, 1999; *Sarnthein et al.*, 2001]. After 22,000 years BP, the $\delta^{18}O$ records show a stable phase, the LIM, lasting until 18,000 years BP, where maximum $\delta^{18}O$ oscillations do not exceed 0.3‰. Slightly larger fluctuations of 0.6‰ occur only in the northernmost core MD 95-2012 (Figure 2e). The stable LIM ended near 18,000 years BP, as indicated by highly depleted $\delta^{18}O$ values that mark the onset of deglaciation during H1.

[25] In core 23415 (Figure 2a), located in the so-called "Heinrich belt" [*Grousset et al.*, 1993], IRD maxima are confined to the Heinrich events. During the LGM and most of MIS 2, the IRD content was as low as during DO interstadials. Sea surface salinity then was high enough that short-term SST increases (e.g., 29,000–26,000 years BP) were compensated for in the $\delta^{18}O$ record. Minor increases in IRD only preceded two short-term intraLGM warmings near 20,000 and 18,500 years BP. At the Iceland-Faroe Ridge, two similar IRD maxima occur at 21,000–20,200, and at 19,500–19,000 years BP. In the Norwegian Sea the IRD levels remained generally high. Nevertheless, distinct IRD minima occur right after H3, along with DO interstadials 4 and 3, when the IRD content abruptly dropped twice

from >90% to 20–40% at the Vøring Plateau and to 50% off northern Norway. IRD levels also dropped to 50–70% right after H2, during interstadial DO 2, and immediately prior to H1 (Figures 2c and 2e). Near 14,500 years BP, at the onset of the Bølling interstadial, the IRD content started to decline toward zero in both the northeast Atlantic and the Norwegian Sea, except for the northernmost site MD 95-2012.

[26] The most pronounced variations in the planktonic fauna and SST occurred in the northeast Atlantic (core 23415, Figure 2a). Here the three techniques yielded similar SST estimates with regard to both the absolute level and the curve trend. Northeast Atlantic SST during MIS 2 varied between 3.5° and 9°C (SIMMAX), 2° and 9°C (RAM), and 3° and 8.5°C (ANN). The abundance of the polar species *N. pachyderma* sin. varied between 50 and 95% (Figure 2a). Distinct warmings occurred after Heinrich events 3 and 2, respectively, at 29,000–26,700 (spanning DO 4 and 3) and 23,700–23,000 years BP (DO 2). Warmings also occurred twice during the LIM with short increases to 6–7°C, near 20,800–20,300 years and ~19,000–18,000 years BP. These additional SST excursions are not reflected in the uniform $\delta^{18}O$ record defining the LIM and therefore suggest compensation by short-term salinity increases of 1–2 psu (as also assumed by *Rosell-Melé et al.* [2002]). These LGM warmings were less prominent than the preceding DO interstadials during MIS 3 and early MIS 2, but lasted 500–800 years each and were spaced about 1500 years apart, precisely as other earlier DO events [*Grootes and Stuiver*, 1997]. Their occurrence in the middle and at the end of the LGM roughly coincides with two minor warmings in the GISP2 record near 18,000 and 19,300 years BP [*Stuiver and Grootes*, 2000].

[27] At the southern Iceland Faroe Ridge (cores 16396/97, Figure 2b), SST estimates range between 3° and 8°C (SIMMAX), 2° and 7°C (ANN), and 0.5° and 9°C (RAM). By and large the general pattern of SST variation is reproduced by all three techniques. As would be expected because of its calibration to temperature in the 0–75 depth range, ANN yields slightly lower absolute values, whereas RAM estimates show a number of additional, large-magnitude fluctuations, especially between 20,000 and 18,000 years BP. Similar to core 23415, warm SST of 5–7°C mark DO interstadial 2 subsequent to H2, over the interval 23,400–22,500 years BP. A more pronounced warm excursion, reaching estimates of 7–9°C, after H3 is disrupted by a hiatus (28,700–26,500 years BP). A second hiatus spans the late H1 and Bølling, subsequent to 16,500 years BP. These erosional gaps during the most prominent DO interstadials can perhaps be attributed to vigorous overflow of Norwegian Sea Deepwater. Today the overflow forms a contour current along the southern flank of the IFR, preventing any sediment deposition [*Dorn and Werner*, 1993].

[28] Unlike the record of core 23415, no distinct centennial-scale warm events are found at the Iceland Faroe Ridge during the LIM, although minor SST changes of 1–2°C occurred at higher frequency in harmony with the percentage fluctuations of *N. pachyderma* sin. (variation of about 3%). These minor variations are likewise depicted in the smooth SIMMAX and ANN records (Figure 2b). SIMMAX-based SST exceeding 4°C (matched by <95% abundance of polar *N. pachyderma* sin.) suggest repeated incursions of warm Atlantic surface water. Such incursions are concentrated in the interval after 20,000 years BP and predate the early onset of deglaciation at ~18,700 years BP. At the same time the IRD content reached a minimum, indicating that icebergs disappeared from this area (Figure 2b).

[29] In the Norwegian Sea SST variability was extremely low during MIS 2. In cores 23071 and 23074 (Figures 2c and 2d) off mid Norway, both the SIMMAX and ANN techniques reconstruct SST fluctuations of less than 1°C amplitude (2.7°–3.8°Cand 2.5°–3.5°C, respectively). A slightly higher variability of 1.7°C occurs at the northernmost site MD 9520-12 (Figure 2e). Here SST minima of <2°C mark the end of H2 (23,000–22,500 years) and at ~22,000, 21,500, and 20,500 years BP. The only warmer episodes in the Norwegian Sea occurred subsequent to H2 at DO interstadial 2, at ~23,500–23,000 years BP (cores 23074 and MD 95-2012), and also at the Bølling interstadial, when SST reached 4.5°C and the abundance of *N. pachyderma* sin. decreased abruptly to<95–90% (cores 23074 and MD 95-2012).

3.2. Reliability of Cold SST Estimates

[30] In the temperature range near the "cold end" RAM estimates clearly deviate from SIMMAX and ANN estimates, with the magnitude of centennial-scale variations being much larger (1°/2°C–6°C). In general, the SIMMAX and ANN-based SST patterns (if any) are similar, but ANN estimates are systematically lower, by about 1°C (as expected from the different water depths the two techniques were calibrated to).

[31] The small magnitude of SIMMAX and ANN-based SST variations is consistent with 0.3‰ fluctuations around the near constant high planktonic $\delta^{18}O$ level of 4.5–4.8‰ and implies a long-term stable sea surface salinity (SSS) without major meltwater incursions. In contrast, the RAM SST fluctuations of 4°–6°C would suggest ongoing rapid salinity fluctuations as high as 3 psu in the glacial Norwe-

Figure 2. (opposite) $\delta^{18}O$ (*Neogloboquadrina pachyderma* sin.), IRD percentage (of total coarse fraction >150 μm), *N. pachyderma* sin. percentage, and SST records (summer SST only) based on different transfer technique (SIMMAX, ANN, and RAM, from top to bottom). Numbers in the upper panels are ^{14}C ages (corrected for 400-year reservoir age), used as age control points subsequent to a calibration to the calendar timescale (see Table 1). Horizontal lines are provided to ease intercomparison of SST estimates. (a) Core 23415 (insert graph shows correlation of all SIMMAX- and ANN-based SST estimates depicted in Figures 2a–2e). (b) Cores 16396/16397. (c) Core 23071. (d) Core 23074. (e) Core MD 95-2012. Oxygen isotopes, selected ^{14}C dates, and IRD from *Dreger* [1999]. Details of chronostratigraphy are derived from the correlation of magnetic susceptibility records in core MD 95-2012 (gray curve in second panel) and 95-2010 (stippled gray curve) (M. Pirrung, manuscript in preparation, 2003; M. Pirrung, personal communication, 2002).

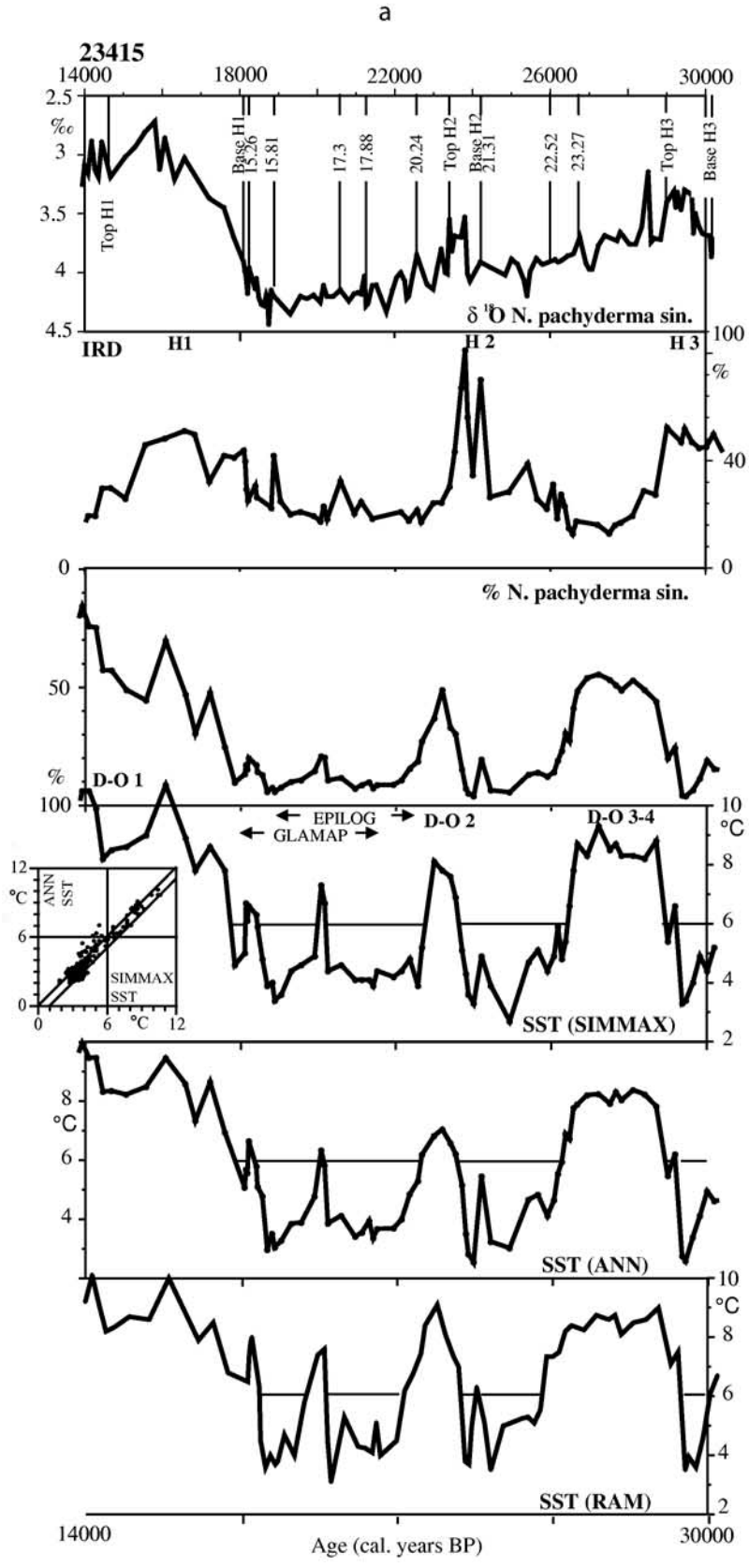
a
23415
14000
18000
22000
26000
30000
2.5
‰
3
3.5
4
4.5
Top H1
Base H1
15.26
15.81
17.3
17.88
20.24
Top H2
Base H2
21.31
22.52
23.27
Top H3
Base H3
δ 18O N. pachyderma sin.
IRD
H1
H 2
H 3
100
%
40
0
% N. pachyderma sin.
50
D-O 1
EPILOG
GLAMAP
D-O 2
D-O 3-4
10
°C
8
6
4
2
12
ANN SST
SIMMAX SST
SST (SIMMAX)
SST (ANN)
SST (RAM)
Age (cal. years BP)

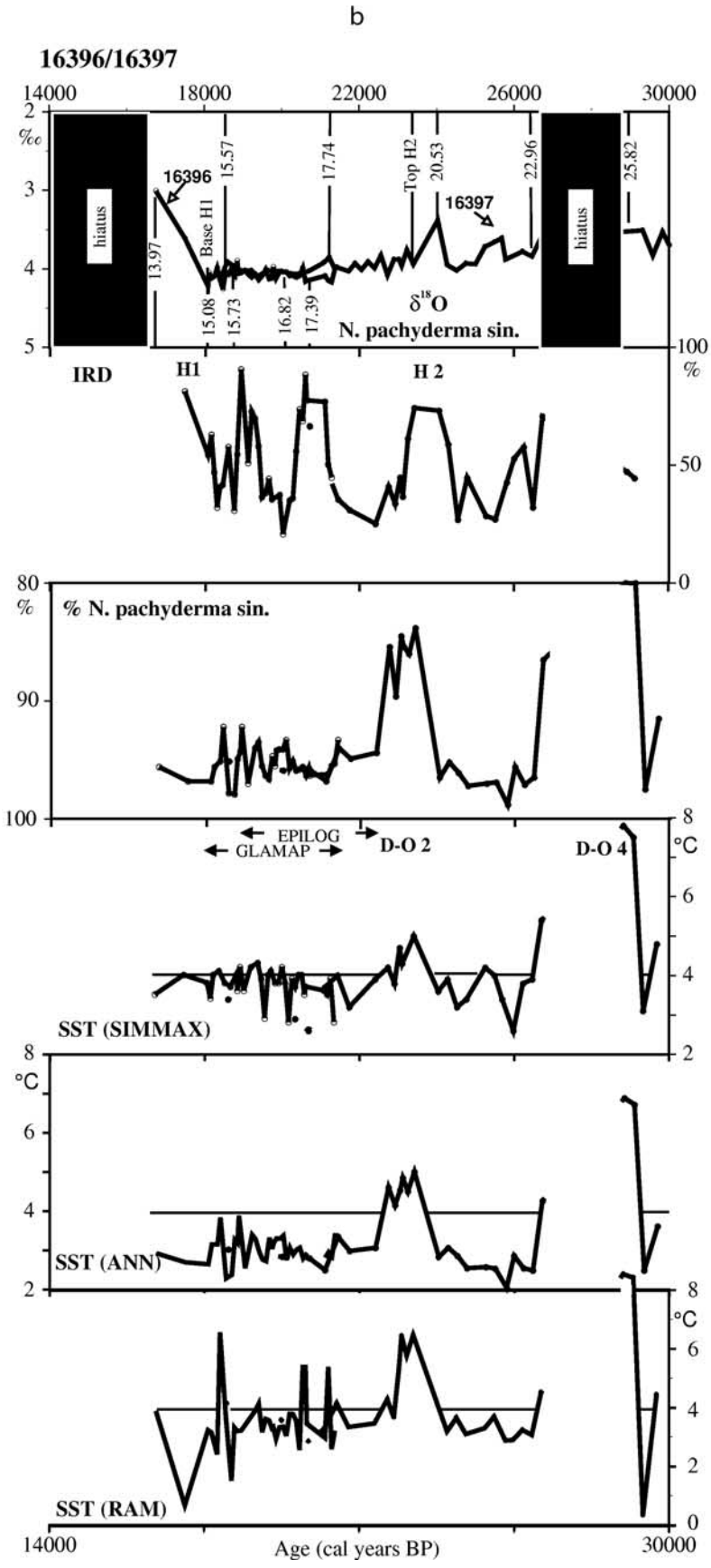

Figure 2. (continued)

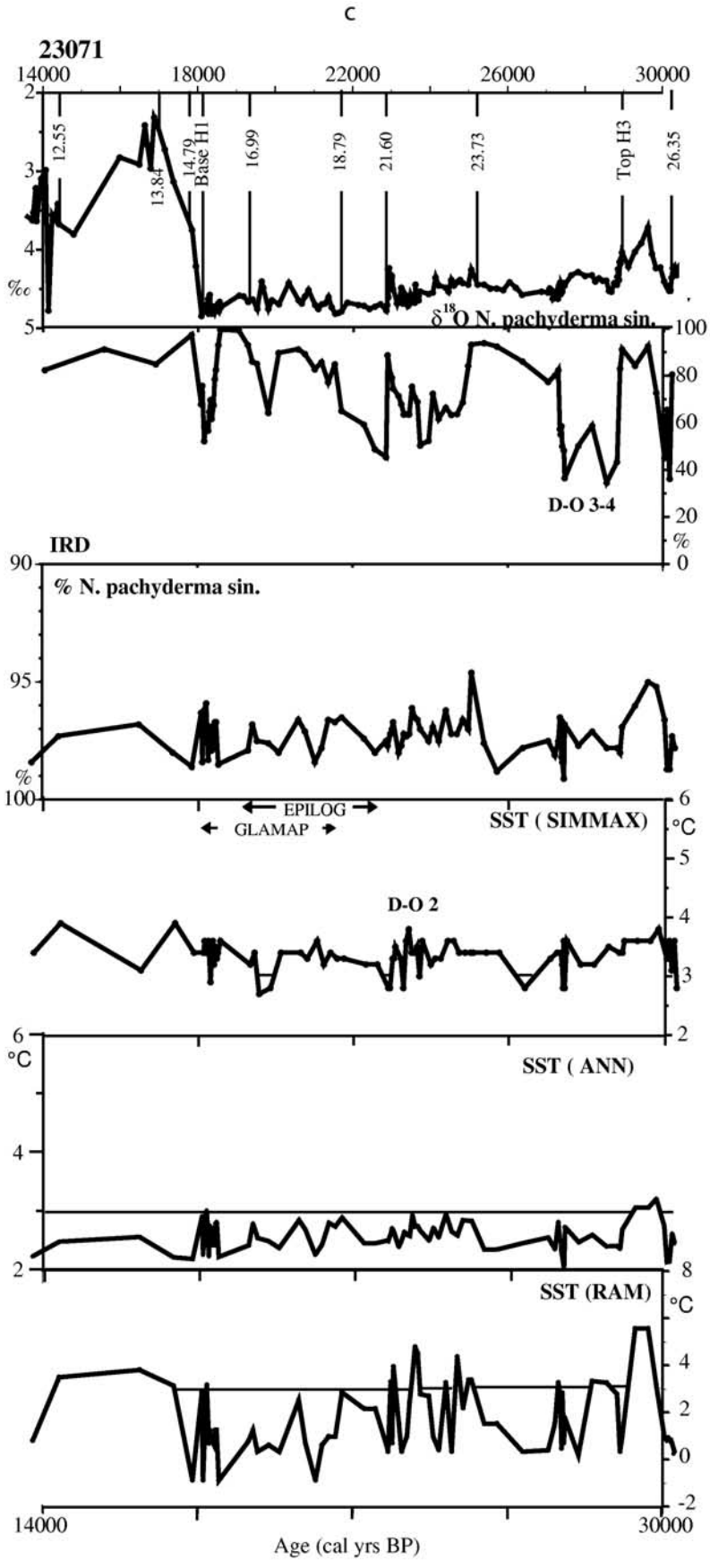

Figure 2. (continued)

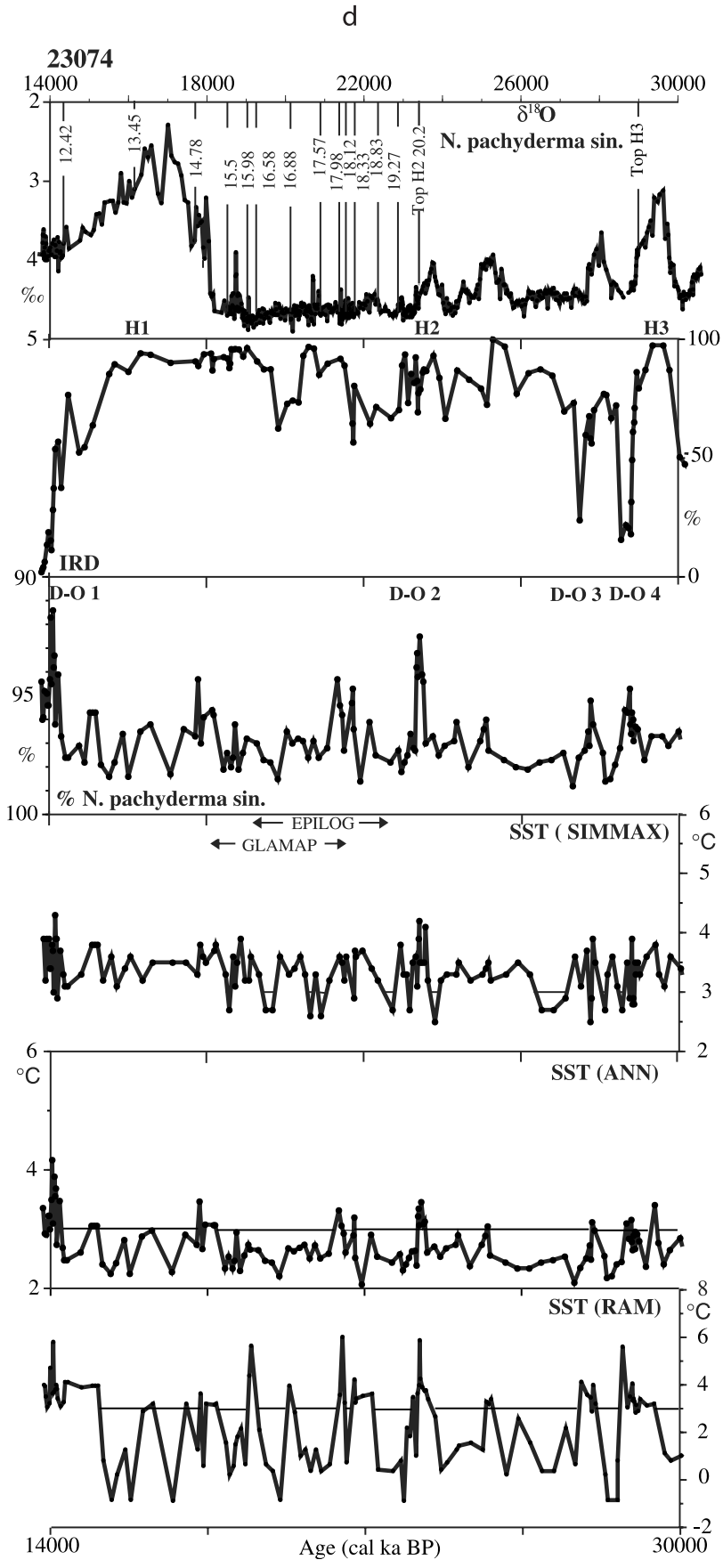

Figure 2. (continued)

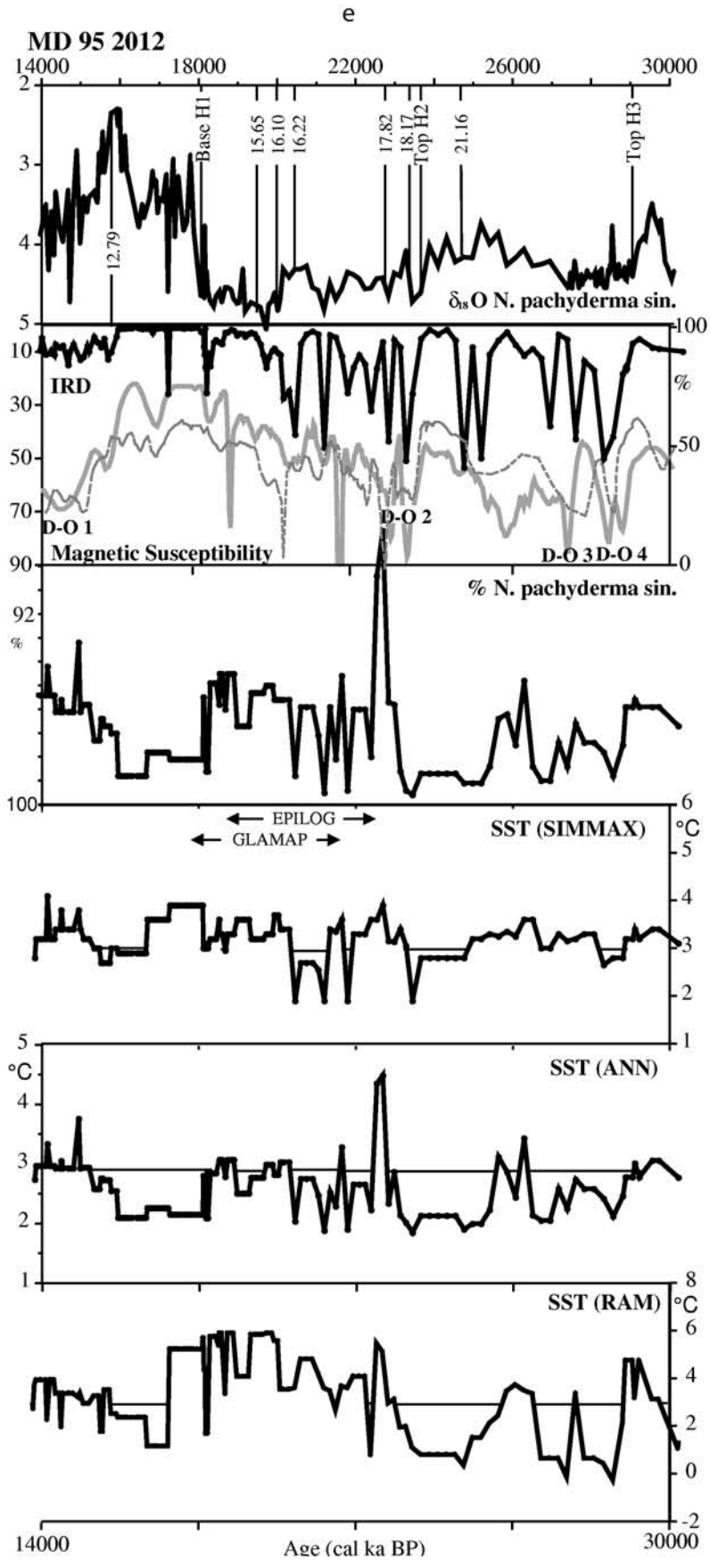

Figure 2. (continued)

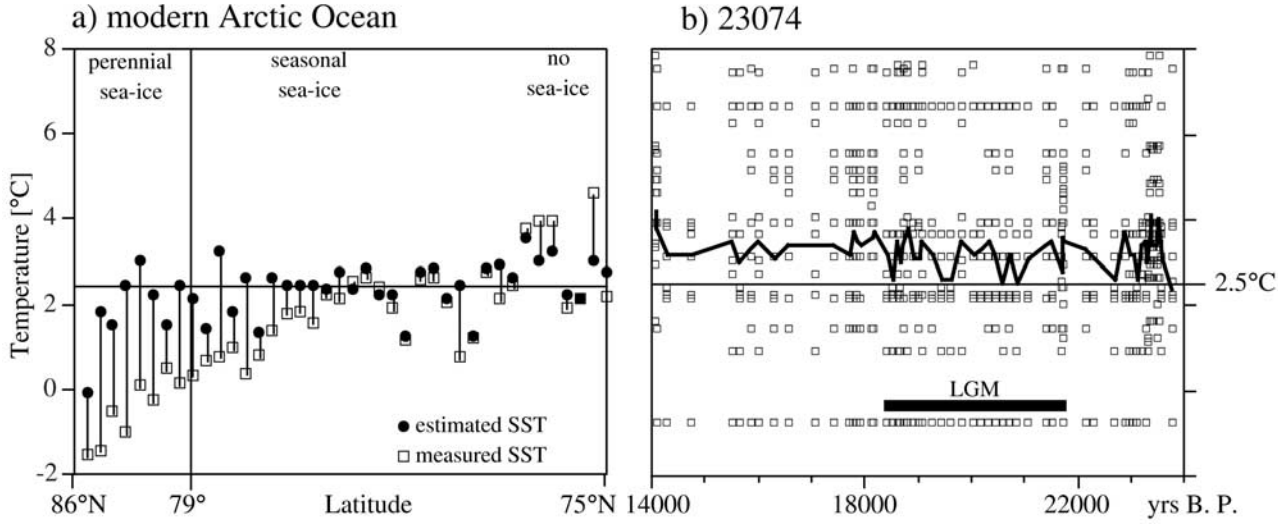

Figure 3. Derivation of past sea ice cover during summer. (a) Measured versus estimated SST values in the Atlantic sector of the Arctic Ocean. SIMMAX SST estimates were derived from core-top samples 79°–85°N. Perennial sea ice does not occur at SIMMAX estimates >2.5°C in 8 out of 9 cases. (b) SIMMAX-based SST estimates (bold line) at Site 23074 for the time span 14–24 ka. In addition, the SST range of 10 modern analog samples (squares) is indicated, which are used by the SIMMAX technique for each temperature estimate. The 2.5°C level that delineates maximum sea ice extent during summer is marked by the horizontal line. Dots and squares in Figure 3a are measured (Levitus, summer, 10 m) and estimated (SIMMAX) SST for core tops. Vertical line marks the limit of perennial ice cover. Solid curve in Figure 3b shows estimated SST (SIMMAX). Open squares are 10 modern analogs selected by SIMMAX for each sample. Horizontal line marks 3°C level as threshold level of estimates beneath perennial sea ice.

gian Sea. This estimate of Δ 3psu is based on the transfer technique of *Duplessy et al.* [1991] assuming a regression slope of 1:2 (‰ δ^{18}O: ‰ SSS) and a depth habitat of *N. pachyderma* sin. of 30–50 m which *Simstich et al.* [2002] have shown characteristic for the Arctic Domain that we regard as best water mass equivalent to the LGM Nordic Seas, where the North Atlantic inflow with its deep *N. pachyderma* habitat did hardly exist. In summary, both the subtle differences in the faunal composition of glacial sediment samples, and the planktonic δ^{18}O values suggest that the large SST changes based on RAM appear to be an artifact of noise that generally marks the "cold end" of RAM estimates rather than a real signal [*Weinelt et al.*, 2001; *Pflaumann et al.*, 2003].

[32] Key evidence to resolve this controversy comes from the choice of the modern analog samples used for SST reconstruction in LGM samples of the Norwegian Sea by both the SIMMAX and RAM techniques (Figure 3b; SIMMAX analogs shown only). These analogs show a broad scatter of temperature values ranging from −1° to 7.5°C and come from regions as different as the Arctic Ocean, the Nordic and Labrador Seas. A warm bias is partly introduced by analogs selected in the Labrador and central Norwegian and Greenland Seas. Here core top faunas with *N. pachyderma* sin. accounting for 96–98% of the assemblage differ only little from polar faunas in the cold East Greenland Current (>98–99% at SST of −1° to 3°C) and tend to underestimate modern summer SST by as much as 1.5°–3.5°C. These sites, when chosen as analog sites, may lead to a relative overestimate of the actual SST. In the SIMMAX estimates, this warm "bias" is mostly compensated by the consistent inclusion of all 10 best analogs and by the distance weighting procedure [*Pflaumann et al.*, 2003]. In contrast, many RAM-based estimates are exclusively derived from only two or three analogs, which results in SST excursions up to 6°C (Figures 2c–2e). The large and abrupt SST jumps based on RAM may therefore be an artifact of the restrictive analog selection. This conclusion is reinforced by ANN estimates, which show SST variation of the same magnitude as SIMMAX estimates. Possibly, RAM estimates would be less spurious in case parameter α of RAM was further increased and a broader set of modern analogs selected (C. Waelbroeck, personal communication, 2002).

3.3. Short-Term Variations in Sea-Ice Extent on the Nordic Seas During Glacial Summer

[33] Near the "cold end," that is near and below perennial sea ice, both SIMMAX and ANN tend to overestimate SST [*Sarnthein et al.*, 2003b]. Hence the precise summer temperature near the freezing limit (<1°–0°C according to *Levitus and Boyer* [1994]), which is expected below perennial sea ice (50% coverage; *Gloersen et al.* [1992]), cannot be reproduced by SIMMAX summer estimates, which never decrease below 1.5°C [*Pflaumann et al.*, 2003]. Figure 3a illustrates SIMMAX-based estimates versus measured SST for a meridional transect of core tops from the Arctic Ocean, as compared to the SST record of core 23074 (Figure 3b).

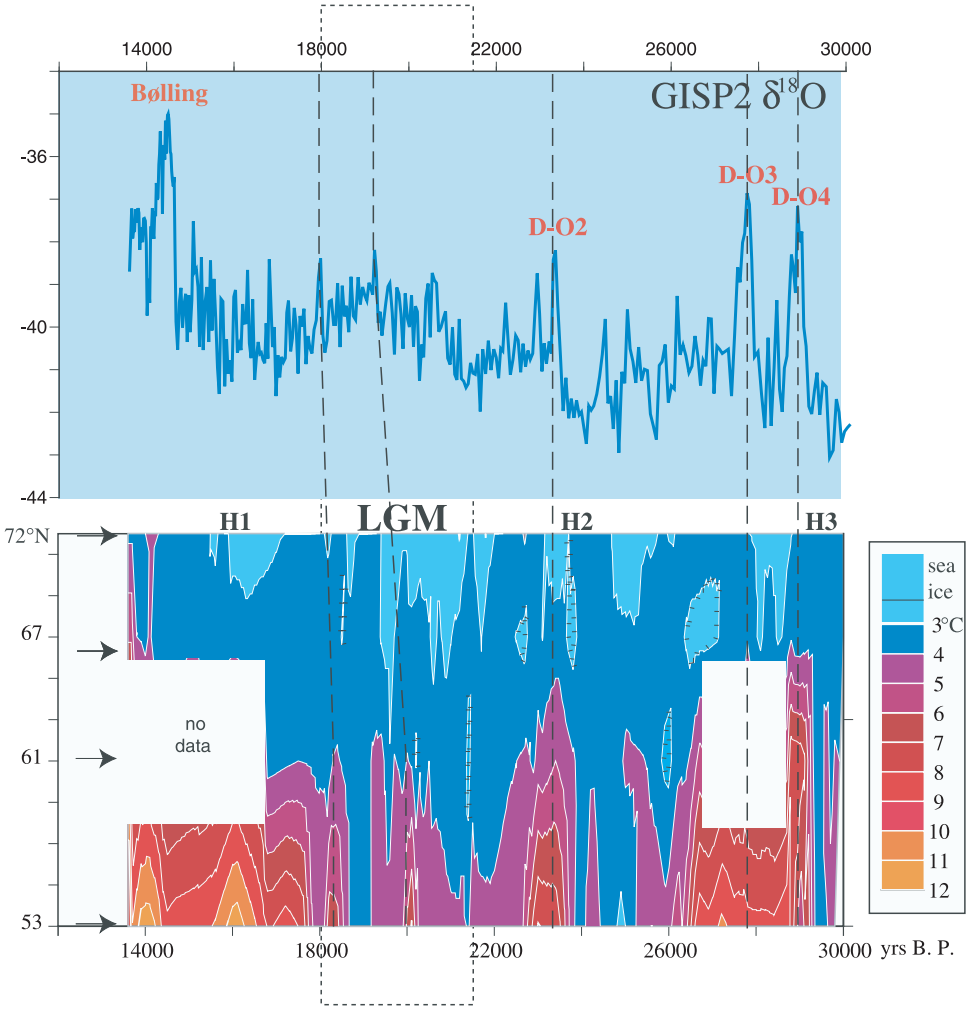

Figure 4. Evolution of the heat transport along the 53–72°N transect over MIS 2 as compared to the GISP2 $\delta^{18}O$ record [*Stuiver and Grootes*, 2000]. Contour map is based on SIMMAX summer SST records in Figure 2, interpolated to 200-year equidistant time steps using linear triangulation. The 2.5°C contour is used as a rough guide to delimit occurrence of perennial ice. Dashed lines connect D-O interstadials in ice and marine records. Tentative correlation lines in the LGM imply that slight improvements in the age models could be achieved with limited tuning.

Using the approach of *Sarnthein et al.* [2003b], we accordingly define the SIMMAX estimate of 2.5°C as the maximum level that will support 50% sea ice cover during summer, and assume (by strict modern analogue) ice-free conditions at any higher SST (no such calibration is yet available for ANN-based SST estimates).

[34] In core 23074 only 5 out of 24 LGM SST estimates and in core 23071 only 3 out of 23 estimates (Figure 2d) fall below the 3°C level over the Vøring Plateau. None of them fall below 2.5°C, the threshold temperature for summer sea ice. The temperature minima occur in the early LGM (21,000–20,500 years BP), coeval with a maximum in IRD-deposition, and later on, at 19,800–19,500 years BP. Perennial ice cover of the Norwegian Sea is excluded for the most of MIS 2, including Heinrich events 2 and 3, when meltwater could have favored freezing. In contrast, our reconstructions suggest that periods of perennial ice were more common at the northernmost site MD 9520-12 (Figure 2e), which lay close to the Barents Ice Sheet during MIS 2 [*Elverhøi et al.*, 1993]. In particular this applies to part of the LGM, where SST estimates below 2.5°C indicate a perennial ice cover for 3 out of 18 LGM samples. Warmer intervals (>3.5°C) only occurred during DO interstadial 2 and also near 18,500 years BP.

3.4. Spatial Pattern of SST Variability During the LGM

[35] The contour graph in Figure 4 provides a (SIMMAX-based) overview of the regional extent of cold waters in the North Atlantic and the Nordic Seas between 26,000 and 18,000 years BP. The cold glacial was disrupted by DO interstadial 2 (23,500–22,500 years BP), when warmer water advection reached up to 67°N. Further, short-lived, interstadial-like warmings occurred south of 61°N at 20,000 and 18,500 years BP. The LGM and H1 appear as end-members of a long-term, saw-tooth style oceanographic

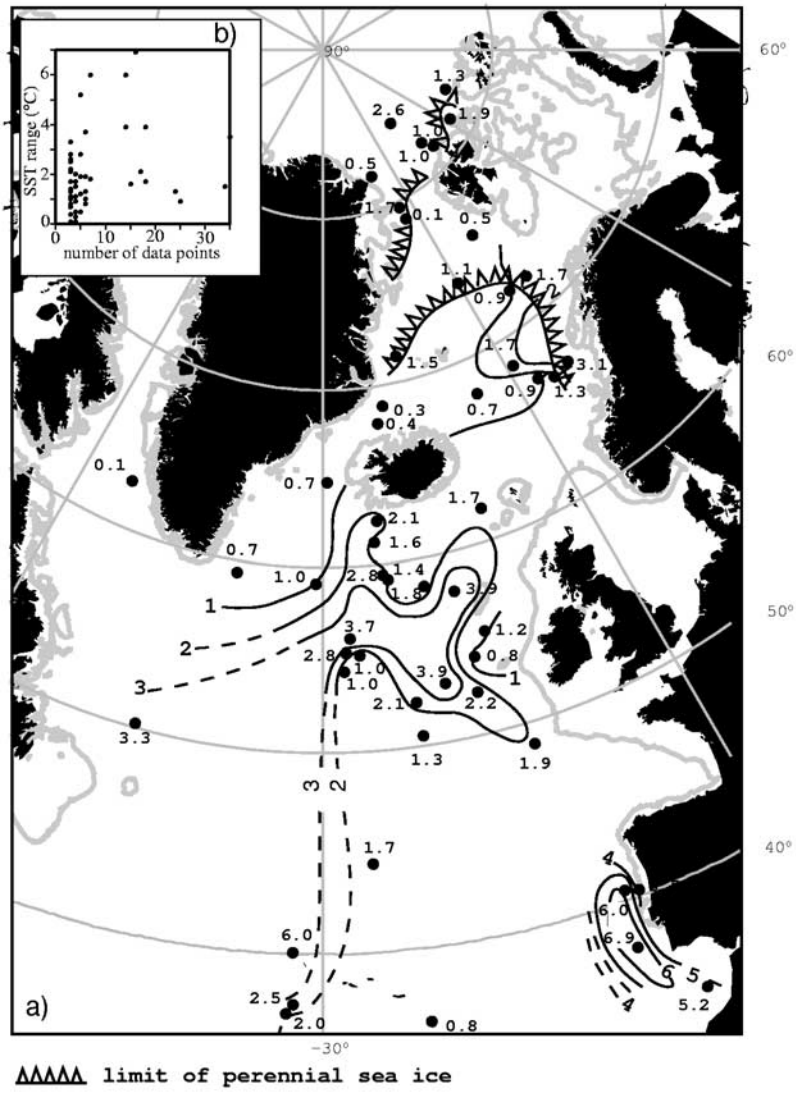

Figure 5. (a) Patterns of North Atlantic SST (summer) variability during the LGM interval (18,000–21,500 years BP) based on the GLAMAP 2000 compilation. Values (in centigrade) are differences between warmest and coldest SST estimates occurring within the LGM interval. Toothed contours are maximum and minimum limits of perennial sea ice (deduced from the 2.5°C isotherm) based on the distribution of coldest and warmest LGM-SST estimates, respectively (Table 2). (b) Number of SST data in LGM records versus observed LGM-SST range showing no systematic correlation.

evolution over MIS 2, where the intensity of warmish episodes has gradually decreased, finally not reaching further than 61°N, the IFR. Thus the DO cyclicity of climate clearly continued over MIS 2, although with warm water only reaching up to the IFR. On land, warm phases are reported up to 70°N [*Paus*, 1990]. The massive cooling of H1 was largely confined north of the IFR. Thus our data suggest that the IFR formed a major climatic barrier during the LGM as predicted by the model of *Ganopolski and Rahmstorf* [2001].

[36] On the basis of a back-of-the-envelope calculation we tried to roughly assess the end-member variations in oceanic poleward heat transfer during MIS 2. For this purpose we (1) regarded the North Atlantic/Norwegian Current as a ''warm-water hose,'' with different reach representing different pressures, as expressed in a south-north SST gradient over more than 2000 km, from 53° to 72°N; (2) assumed the SST variations at critical latitudes, such as on the Iceland Faroe Ridge, to be linearly proportional to the heat transport (for calibration, we set 3°C at 61°N equal to zero transport and 12°C, as measured today, equal to 230 TW [*Hansen et al.*, 2001]; and (3) assumed a constant heat loss to the atmosphere over the complete range of latitudes discussed.

[37] Based on this calculation, the near-surface poleward heat transfer dropped almost to zero at ~29,000 years BP, 25,000–24,000 years BP, and from 23,000 until 16,500 years BP, disrupted only by very minor warm-water incursions with up to 30 TW heat transfer. Consistent with this conclusion, the SST gradient between 53° and 72° dropped

Table 2. Range of SST in North Atlantic Cores During the LGM According to GLAMAP 2000 and EPILOG[a]

			GLAMAP 2000				EPILOG			
Latitude, °N	Longitude	Core Number	Number of Samples	Minimum SST	Maximum ST	SST Range	Number of Samples	Minimum SST	Maximum SST	SST Range
67.959	−18.612	1171-1	1	3.8	3.8	-	2	3.8	4.2	0.4
44.360	**−26.543**	**15612-2**	**4**	**6.9**	**8.6**	**1.7**	**4**	**7.9**	**8.6**	**0.7**
34.892	**−7.8150**	**15669-1**	**5**	**17.3**	**22.5**	**5.2**	**5**	**17.3**	**22.5**	**5.2**
61.867	**−11.250**	**16396-1**	**34**	**2.8**	**4.3**	**1.5**	**24**	**2.8**	**4.3**	**1.5**
61.867	**−11.250**	**16397-2**	**4**	2.6	**3.7**	**1.1**	**7**	**2.6**	**4.0**	**1.4**
52.425	**−16.665**	**17045-3**	**3**	**4.3**	**6.5**	**2.2**	1	6.5	6.5	-
55.267	**−26.733**	**17049-6**	**3**	**3.4**	**4.4**	**1.0**	2	3.4	4.1	0.7
55.470	**−27.888**	**17050-1**	**3**	**5.0**	**7.8**	**2.8**	**3**	**5.0**	**7.8**	**2.8**
56.163	−31.990	17051-3	1	4.5	4.5	-	1	4.3	4.3	-
76.000	**8.3333**	**17724-2**	**4**	**2.3**	**2.8**	**0.5**	**5**	**2.3**	**2.8**	**0.5**
77.467	4.5833	17725-1	2	2.8	3.1	0.3	1	3.1	3.1	-
72.112	**7.3167**	**17730-4**	**4**	**2.8**	**3.7**	**0.9**	**8**	**2.3**	**3.8**	**1.5**
82.032	**15.178**	**21533-3**	**3**	**1.4**	**2.4**	**1.0**	**4**	**0.5**	**2.4**	**1.9**
68.502	3.8383	23056-2	2	3.6	4.3	0.7	2	3.6	4.3	0.7
68.500	**0.8167**	**23065-2**	**3**	**3.3**	**5.0**	**1.7**	**3**	**3.3**	**5.0**	**1.7**
67.083	**2.9167**	**23071-3**	**25**	**2.7**	**3.6**	**0.9**	**22**	**2.7**	**3.6**	**0.9**
66.667	**4.9050**	**23074-1**	**24**	**2.6**	**3.9**	**1.3**	**21**	**2.6**	**3.7**	**1.1**
72.233	14.433	23262-2	2	3.2	3.5	0.3	2	3.2	3.5	0.3
72.750	−10.6	23294-4	2	3.2	3.3	0.1	1	3.2	3.2	-
70.358	−18.217	23351-1	1	3.4	3.4	-	1	3.4	3.4	-
70.332	−10.628	23354-6	1	3.5	3.5	-	1	3.5	3.5	-
53.173	**−19.2**	**23415-9**	**18**	**3.2**	**7.1**	**3.9**	**18**	**3.2**	**7.1**	**3.9**
54.960	−19.750	23419-8	1	5.2	5.2	-	1	5.2	5.2	-
64.799	**−29.596**	**23519-5**	**3**	**2.9**	**3.6**	**0.7**	**3**	**2.9**	**3.7**	**0.8**
50.683	**−21.867**	**BOFS05KA**	**6**	**3.2**	**4.5**	**1.3**	**10**	**3.2**	**4.5**	**1.3**
52.50	**−22.067**	**BOFS08A**	**17**	**2.7**	**4.8**	**2.1**	**18**	**2.7**	**4.8**	**2.1**
58.617	**−19.433**	**BOFS14**	**7**	**4.1**	**5.9**	**1.8**	**6**	**5.0**	**5.9**	**0.9**
59.280	**−23.140**	**BOFS16K**	**3**	**4.9**	**6.3**	**1.4**	**2**	**4.9**	**6.3**	**1.4**
58.000	**−16.5**	**BOFS17**	**14**	**4.0**	**7.9**	**3.9**	**16**	**4.2**	**8.2**	**4.0**
43.465	−30.660	CH82-24	2	11.5	15.3	3.8	1	11.5	11.5	-
62.648	**−53.884**	**HU87033-**	**4**	**3.1**	**3.2**	**0.1**	**5**	**3.1**	**4.8**	**1.7**
58.210	−48.373	HU90-013	1	3.4	3.4	-	1	3.4	3.4	-
50.330	**−45.686**	**HU91-04**	**3**	**2.9**	**6.2**	**3.3**	**4**	**2.9**	**6.2**	**3.3**
37.111	**−32.287**	**KF09**	**4**	**19.9**	**21.9**	**2.0**	**3**	**21.2**	**21.9**	**0.7**
37.578	**−31.842**	**KF13**	**3**	**18.2**	**20.7**	**2.5**	2	20.4	20.7	0.3
37.999	−31.128	KF16	1	18.0	18.0	-	1	18.0	18.	-
50.000	−23.750	KN708-1	1	2.9	2.9	-	1	2.9	2.9	-
72.151	**11.434**	**MD2012**	**18**	**1.9**	**3.1**	**1.2**	**12**	**1.9**	**3.3**	**1.4**
40.579	**−10.349**	**MD2039**	**7**	**11.5**	**17.5**	**6.0**	**5**	**11.5**	**16.6**	**5.1**
40.350	**−9.52**	**MD2040**	**35**	**14.7**	**18.2**	**3.5**	**42**	**14.1**	**18.2**	**4.1**
55.500	**−14.583**	**NA8722**	**5**	**3.7**	**4.9**	**1.2**	**7**	**3.7**	**4.9**	**1.2**
56.220	**−27.490**	**NEAP15K**	**6**	**4.1**	**7.8**	**3.7**	**6**	**4.1**	**7.8**	**3.7**
54.410	**−28.210**	**NEAP17K**	**3**	**4.3**	**5.3**	**1**	**4**	**4.3**	**6.8**	**2.5**
62.500	**−23.570**	**NEAP3K**	**3**	**2.1**	**4.2**	**2.1**	**3**	**2.1**	**4.2**	**2.1**
61.300	**−24.1**	**NEAP4K weg**	**15**	**3.2**	**4.8**	**1.6**	**15**	**3.2**	**4.8**	**1.6**
59.470	**−23.540**	**NEAP8K**	**5**	**5.4**	**8.2**	**2.8**	**5**	**5.4**	**8.2**	**2.8**
84.029	**11.238**	**OD41-4-1**	**3**	**−0.8**	**1.8**	**2.6**	**2**	**−0.80**	**1.4**	**2.2**
49.050	**−13.260**	**OMEX2K**	**6**	**4.1**	**6.0**	**1.9**	**4**	**4.1**	**6.0**	**1.9**
78.858	**−4.7750**	**PS1230-1**	**3**	**1.0**	**1.1**	**0.1**	**2**	**1.0**	**1.1**	**0.1**
70.120	−17.702	PS1730-2	1	3.4	3.4	-	1	3.5	3.5	-
74.997	−11.903	PS1919-2	1	2.7	2.7	-	2	2.7	2.9	0.2
75.000	−8.7717	PS1922-1	2	2.2	2.3	0.1	2	2.2	2.7	0.5
71.496	**−17.118**	**PS1927-2**	**4**	**2.2**	**3.7**	**1.5**	**3**	**2.2**	**3.7**	**1.5**
68.842	**−20.820**	**PS1951-1**	**4**	**3.4**	**3.7**	**0.3**	**3**	**3.4**	**3.7**	**0.3**
81.367	**17.472**	**PS2129-1**	**3**	**1.0**	**2.0**	**1.0**	2	1.0	1.7	0.70
81.535	**30.593**	**PS2138-1**	**5**	**0.80**	**2.7**	**1.9**	**4**	**2.1**	**2.7**	**0.6**
82.397	**40.908**	**PS2446-4**	**3**	**1.0**	**2.3**	**1.3**	**3**	**1.0**	**2.3**	**1.3**
74.176	**−0.47880**	**PS2613-6**	**3**	**2.8**	**3.9**	**1.1**	2	3.1	3.9	0.8
67.867	**−21.765**	**PS2644-5**	**3**	**3.2**	**3.6**	**0.4**	2	3.2	3.3	0.1
81.233	2.3833	PS2837-5	2	0.80	1.2	0.4	**3**	**0.70**	**1.2**	**0.5**
81.908	**−9.4350**	**PS2876-1**	**5**	**2.1**	**2.6**	**0.5**	**4**	**2.1**	**2.6**	**0.5**
79.600	**−4.6083**	**PS2887-1**	**3**	**0.80**	**2.5**	**1.7**	**3**	**0.80**	**2.5**	**1.7**
59.168	**−30.905**	**SO82-5**	**6**	**3.4**	**4.4**	**1.0**	**20**	**2.3**	**9.1**	**6.8**
37.767	**−10.783**	**SU81-18**	**16**	**13.**	**19.9**	**6.9**	**15**	**9.6**	**19.9**	**10.3**
40.000	**−32.000**	**SU90-03**	**14**	**12.3**	**18.3**	**6.0**	**10**	**15.6**	**18.3**	**2.7**
52.567	−21.933	SU90-39	2	3.9	4.3	0.4	**3**	**3.9**	**4.3**	**0.4**
59.445	**−39.522**	**SU90I06**	**3**	**3.5**	**4.2**	**0.7**	**2**	**3.5**	**4.2**	**0.7**
36.512	**−23.744**	**SU92_21**	**3**	**19.8**	**20.6**	**0.8**	2	19.8	20.6	0.8

Table 2. (continued)

			GLAMAP 2000				EPILOG			
Latitude, °N	Longitude	Core Number	Number of Samples	Minimum SST	Maximum ST	SST Range	Number of Samples	Minimum SST	Maximum SST	SST Range
54.250	**−16.133**	**V23-081**	**6**	**4.4**	**5.2**	**0.8**	**4**	**4.4**	**4.4**	**0.0**
72.183	8.580	V27-60	2	3.2	3.2	0.0	1	3.2	3.2	-
66.600	−1.1166	V27-86	2	3.6	9.5	5.9	2	3.0	3.6	0.6
64.783	**−29.567**	**V28-14**	**3**	**3.5**	**4.2**	**0.7**	2	3.9	4.2	0.3
68.033	**−6.1166**	**V28-56**	**3**	**3.6**	**4.3**	**0.7**	**3**	**3.6**	**4.3**	**0.70**
44.010	−24.540	V29-179	1	9.0	9.0	-	2	9.0	13.4	4.4

[a]Records where the LGM is represented by 3 or more data points in bold.

nearly to zero during these times. In contrast, the glacial heat transport increased to 130/110 TW during DO interstadials 4, 3, 2. At the same time the south-north SST gradient increased up to 4°C between 61° and 72°N, indicating an "enhanced pressure in the North Atlantic warm water hose." In summary, the glacial poleward heat transport was probably reduced to somewhere between 0 and 60 percent of the modern value.

[38] The spatial variability of SIMMAX-based SST over the North Atlantic during glacial summer is inferred from mapping the range of SST amplitudes which are contained in the GLAMAP 2000 data set (north of the latitude of Gibraltar) [*Pflaumann et al.*, 2003] (Figure 5a, Table 2). However, the amplitudes of short-lived warm or cool fluctuations registered in a sediment record may in part depend on the temporal resolution of the record. Following *Mix et al.* [2001] we thus consider only records where the LGM is represented by three or more SST estimates (Table 2). Here the SST range indeed does not correlate with the number of data points per LGM record (Figure 5a). The pattern shown in Figure 5a thus largely reflects the actual spatial variability of SST during the LGM.

[39] Maximum temperature variability predominantly emerges in two regions: (1) along the Iberian margin (ΔSST 6°–7°C), where a strong cooling marked the late LGM (Table 2, cores 15669, MD 9520-39/40, SU 81-18; *Vogelsang et al.* [2001]), (2) in the central midlatitude North Atlantic (ΔSST 3.5–4°C) near the northern and eastern margin of an anticyclonic subpolar gyre which developed during the LGM [*Pflaumann et al.*, 2003]. Here intraLGM SST amplitudes come close to the SST difference between DO stadials and interstadials [*Van Kreveld et al.*, 2000]. Several sites record an upper extreme of SST reaching 6–8°C (Table 2), such as the high-resolution core 23415 (Figure 2a). The Nordic Seas apparently display greater SST stability (Figure 5a), with LGM SST amplitudes of ∼1°C and less, as is the case in cores 23071 and 23074 (Figures 2c and 2d). Toward Fram Strait, as in core MD 95-2012 (Figure 2e), the variability exceeds 1.5°C, because minimum SST drops to <2°C (Table 2). In part, this stability may be spurious, since below 2.5°C the SIMMAX temperature estimates (such as ANN estimates) tend to overestimate SST by up to 3.5°C (Figure 3).

[40] On the basis of the 2.5°C isotherm, Figure 5a also shows that the inferred limits of summer sea ice (Figure 5a) varied between 70/74°N and 77/80°N, under the assumption that short-term cold or warm fluctuations were coeval over the entire region. Accordingly, during the coldest LGM intervals the perennial ice margin extended along the Scandinavian continental ice sheet and along the Greenland ice sheet down to the Scorseby Sound (70°N), leaving the central Nordic Seas open. During the warmest LGM intervals perennial sea ice was confined to the western Fram Strait and the Arctic Ocean, a pattern similar to modern winter conditions [*Gloersen et al.*, 1992]. For any LGM scenario, the central Nordic Seas remained ice-free, while the western Fram Strait and the adjacent Arctic Ocean remained permanently ice-covered, in harmony with the reconstruction by *De Vernal et al.* [2000].

4. Conclusions

[41] Amongst three independent techniques used to derive paleotemperatures, the SIMMAX and ANN methods reproduced SST fluctuations of similar magnitude and absolute levels in northern North Atlantic records of MIS 2. As expected from the differing water depth range used for calibration, ANN-based temperatures are ∼1°C colder than SIMMAX-based temperatures. RAM ($\alpha = 0.5$, $\beta = 10$, $\gamma = 0.4$ $R = 0.5$°C), due to its restrictive analog selection, appears oversensitive to small fluctuations in "cold" faunas, producing a high-amplitude noise in "cold-end" SST reconstructions.

[42] Dansgaard-Oeschger cyclicity continued in the northeast Atlantic over MIS 2. We identified two warming phases by 3–5°C, which are spaced by ∼1500 years and were reproduced by all three SST reconstruction techniques. These incursions of warm water did not extend north of the Iceland Faroe Ridge. Simple calculations suggest that the poleward heat transfer across the Iceland-Faroe Ridge linked to the North Atlantic/Norwegian Current System dropped from a modern value of 230 TW to approximately 50% (130–110 TW) of the modern value during D-O interstadials and to almost zero during stadial/full glacial conditions.

[43] During the LGM, a broad range of SST variability (3°–6°C) marks the Iberian Margin and the subpolar North Atlantic. Fairly stable temperatures prevailed in the Nordic Seas, where SIMMAX and ANN estimates suggest continuously cold SST of 2.5–4°C, possibly biased by an overestimation of SST.

[44] Sea ice in the Nordic Seas, however, was the exception rather than the rule during the LGM summers and was confined to the margins. The central parts of the Norwegian-Greenland Seas remained permanently ice-free. In contrast, the adjacent Arctic Ocean was permanently ice covered.

[45] **Acknowledgments.** We are grateful to SFB 313, IMAGES I, and BMBF who funded this study. Michal Kucera was supported by the Nuffield Foundation. Michael Pirrung kindly provided us with his detailed stratigraphic correlation between MD sites 95-2010 and 95-2012, based on magnetic susceptibility. We thank Larry Peterson and two anonymous referees for their constructive comments.

References

Blunier, T., et al., Asynchrony of Antarctic and Greenland climate during the last glacial period, *Nature*, *394*, 739–743, 1998.

Bond, G., W. Broecker, S. Johnsen, J. Mc Manus, L. Labeyrie, L. Jouzel, and G. Bonani, Correlations between climate records from the North Atlantic sediments and Greenland ice, *Nature*, *365*, 143–147, 1993.

Broecker, X., Thermohaline circulation, the Achilles heel of our climate system: Will man made CO2 upset the current balance?, *Science*, *278*, 1582–1588, 1997.

Carstens, J., and G. Wefer, Distribution of planktic foraminifera at the ice-margin in the Arctic (Fram Strait), *Mar. Micropaleontol.*, *29*, 257–269, 1997.

Charles, C. D., D. Rind, J. Jouzel, R. D. Koster, and R. G. Fairbanks, Glacial-interglacial changes in moisture sources for Greenland: Influences on the ice core record of climate, *Science*, *263*, 508–511, 1994.

CLIMAP Project Members, The surface of the Ice-Age Earth: Quantitative geological evidence is used to reconstruct boundary conditions for the climate 18,000 years ago, *Science*, *191*, 1131–1137, 1976.

CLIMAP Project Members, Seasonal reconstruction of the Earth's surface at the last glacial maximum, *Map and Chart Ser., MC-36*, Geol. Soc. of Am., Boulder, Colo., 1981.

Dansgaard, D., et al., Evidence for general instability of past climate from a 250-kyr ice-core record, *Nature*, *364*, 218–220, 1993.

Darling, K. F., C. M. Wade, I. A. Steward, D. Kroon, R. Dingle, and A. J. Leigh Brown, Molecular evidence for genetic mixing of Arctic and Antarctic subpolar populations of planktonic foraminifers, *Nature*, *405*, 43–47, 2000.

De Vernal, A., C. Hillaire-Marcel, J.-L. Turon, and J. Matthiessen, Reconstruction of sea-surface temperature, salinity, and sea-ice cover in the northern North Atlantic during the last glacial maximum based on dinocyst assemblages, *Can. J. Earth Sci.*, *37*, 725–750, 2000.

Dokken, T., and E. Jansen, Rapid changes in the mechanism of ocean convection during the last glacial period, *Nature*, *401*, 458–461, 1999.

Dorn, W. U., and F. Werner, The contour-current flow along the southern Iceland-Faroe Ridge as documented by its bedforms and asymmetrical channel fillings, *Sediment. Geol.*, *82*, 47–59, 1993.

Dowdeswell, J. A., A. Elverhøi, J. T. Andrews, and D. Hebbeln, Asynchronous deposition of ice-rafted layers in the Nordic seas and North Atlantic Ocean, *Nature*, *400*, 348–351, 1999.

Dreger, D., Decadal-to-centennial-scale sediment records of ice advance on the Barents shelf and meltwater discharge into the northeastern Norwegian Sea over the last 40 kyr, PhD thesis, 71 pp., Univ. of Kiel, Kiel, 1999.

Duplessy, J.-C., L. Labeyrie, A. Juillet-Leclerc, F. Maitre, J. Duprat, and M. Sarnthein, Surface salinity reconstruction of the North Atlantic Ocean during the last glacial maximum, *Oceanol. Acta*, *14*, 311–324, 1991.

Elverhoi, A., W. Fjeldskaar, A. Solheim, M. Nyland-Berg, and L. Russwurm, The Barents Sea ice sheet–A model of its growth and decay during the last ice maximum, *Quat. Sci. Rev.*, *12*, 863–873, 1993.

Fronval, T., E. Jansen, J. Bloemendal, and S. Johnsen, Oceanic evidence for coherent fluctuations in Fennoscandian and Laurentide ice sheets on millenium timescales, *Nature*, *374*, 443–446, 1995.

Ganopolski, A., and S. Rahmstorf, Rapid changes of glacial climate simulated in a coupled climate model, *Nature*, *409*, 153–158, 2001.

Gloersen, P., W. J. Campbell, D. J. Cavalieri, J. C. Comiso, C. L. Parkinson, and H. J. Zwally, Arctic and Antarctic Sea Ice, 1978–1987: Satellite passive-microwave observations and analysis, *NASA Spec. Publ.*, *511*, 283 pp., 1992.

Grootes, P. M., and M. Stuiver, Oxygen 18/16 variability in Greenland snow and ice with 10-3 to 105-year time resolution, *J. Geophys. Res.,*, *102*, 26,455–26,470, 1997.

Grousset, F. E., L. Labeyrie, J. A. Sinko, M. Cremer, G. Bond, J. Duprat, E. Cortijo, and S. Huon, Patterns of ice-rafted detritus in the glacial North Atlantic (40–45°N), *Paleoceanography*, *8*, 175–192, 1993.

Hansen, B., W. R. Turrell, and S. Østerhus, Decreasing overflow from the Nordic seas into the Atlantic Ocean through the Faroe Bank channel since 1950, *Nature*, *411*, 927–930, 2001.

Hebbeln, D., T. Dokken, E. S. Andersen, M. Hald, and A. Elverhoi, Moisture supply for northern ice-sheet growth during the last glacial Maximum, *Nature*, *370*, 357–360, 1994.

Hutson, W. H., Transfer functions under no-analog conditions: Experiments with Indian Ocean planktonic foraminifera, *Quat. Res.*, *8*, 355–367, 1977.

Hutson, W. H., The Agulhas current during the late Pleistocene: Analysis of modern faunal analogs, *Science*, *207*, 64–66, 1980.

Jensen, S., Planktonforaminiferen im Europäischen Nordmeer: Verbreitung und Vertikalfluβ, sowie ihre Entwicklung während der letzten 15 000 Jahre, PhD thesis, 105 pp., Univ. of Kiel, Kiel, 1998.

Johnson, S. J., H. B. Clausen, W. Dansgaard, K. Fuhrer, N. Gundestrup, C. U. Hammer, P. Iversen, J. Jouzel, B. Stauffer, and J. P. Steffensen, Irregular interstadials recorded in a new Greenland ice core, *Nature*, *359*, 311–313, 1992.

Joussaume, S., and K. Taylor, Status of the paleoclimate modeling intercomparison project (PMIP), in *Proceedings of the First International AMIP Scientific Conference*, edited by W. L. Gates, pp. 425–430, Atmos. Model Intercomparison Proj., Monterey, Calif., 1995.

Kutzbach, J. E., P. J. Guetter, P. J. Behling, and R. Selin, Simulated climatic changes: Results of the COHMAP climate-model experiments, in *Global Climates Since the Last Glacial Maximum,* edited by H. E. Wright et al., pp. 24–93, Univ. of Minn. Press, Minneapolis, Minn., 1993.

Levitus, S., and T. P. Boyer, *World Ocean Atlas,* vol. 4, *Temperature,*117 pp., NOAA Atlas DIS, Natl. Oceanogr. Data Cent., Ocean Clim. Lab., Washington, D. C., 1994.

Malmgren, B. A., and U. Nordlund, Application of artificial neural networks to paleoceanographic data, *Palaeogeogr. Palaeoclimatol. Palaeoecol.*, *136*, 359–373, 1997.

Malmgren, B. A., M. Kucera, J. Nyberg, and C. Waelbroeck, Comparison of statistical and artificial neural network techniques for estimating past sea-surface temperatures from planktonic foraminifer census data, *Paleoceanography*, *16*(5), 520–530, 2001.

Meese, D. A., A. J. Gow, R. B. Alley, G. A. Zielinski, P. M. Grootes, M. Ram, K. C. Taylor, P. A. Mayewski, and J. F. Bolzan, The Greenland Ice Sheet Project 2 depth-age scale: Methods and results, *Geophys. Res.*, *102*, 26,411–26,423, 1997.

Mix, A., A. E. Morey, and N. G. Pisias, Foraminiferal faunal estimates of paleotemperature: Circumventing the no-analog problem yields cool ice age tropics, *Paleoceanography*, *14*, 350–359, 1999.

Mix, A., E. Bard, and R. Schneider, Environmental processes of the Ice age: Land, Ocean, Glaciers (EPILOG), *Quat. Sci. Rev.*, *20*, 627–658, 2001.

Paus, A., Late Weichselian and Early Holocene vegetation, climate and floral migration at Utsira, North Rogaland, southwestern Norway, *J. Quat. Res. Nor. Geol. Tidskr.*, *70*, 135–152, 1990.

Pflaumann, U., J. Duprat, C. Pujol, and L. D. Labeyrie, A modern analog technique to deduce Atlantic sea surface temperatures from planktonic foraminifera in deep-sea sediments, *Paleoceanography*, *11*, 15–35, 1996.

Pflaumann, U., et al., Glacial North Atlantic: Sea-surface conditions reconstructed by GLAMAP 2000, *Paleoceanography*, *18*(3), 1065, doi:10.1029/2002PA000774, 2003.

Rossel-Melé, A., E. Jansen, and M. Weinelt, Appraisal of a molecular approach to infer variations in surface ocean water inputs into the North Atlantic during the last 50,000 years, *Global Planet. Change*, *34*(3–4), 143–152, 2002.

Sarnthein, M., et al., Fundamental modes and abrupt changes in North Atlantic circulation and climate over the last 60 ky-Concepts, reconstruction, and numerical modelling, in *The Northern North Atlantic: A Changing Environment*, edited by P. Schäfer et al., pp. 365–410, Springer-Verlag, New York, 2001.

Sarnthein, M., R. Gersonde, S. Niebler, U. Pflaumann, R. Spielhagen, J. Thiede, G. Wefer, and W. Weinelt, Overview of Glacial Atlantic Ocean Mapping (GLAMAP 2000), *Paleoceanography*, *18*(2), 1030, doi:10.1029/2002PA000769, 2003a.

Sarnthein, M., U. Pflaumann, and M. Weinelt, Past extent of sea ice in the northern North Atlantic inferred from foraminiferal paleotemperature estimates, *Paleoceanography*, *18*, doi:10.1029/2002PA000771, in press, 2003b.

Schulz, M., W. H. Berger, M. Sarnthein, and P. M. Grootes, Amplitude variations of 1470-year climate oscillations during the last 100,000 years linked to fluctuations of continental ice mass, *Geophys. Res. Lett.*, *26*, 3385–3388, 1999.

Simstich, J., Die ozeanische Deckschicht des Europäischen Nordmeers im Abbild stabiler Isotope von Kalkgehäusen unterschiedlicher Planktonforaminiferenarten, PhD thesis, 83 pp., Univ. of Kiel, Kiel, 1999.

Simstich, J., M. Sarnthein, and H. Erlenkeuser, Paired $\delta^{18}O$ signals of N. pachyderma (s) and T. quinqueloba show the stratification structure in the high-latitude Atlantic, *Mar. Micropaleontol.*, *912*, 1–19, 2002.

Stuiver, M., and P. M. Grootes, GISP2 oxygen isotope ratios, *Quat. Res.*, *53*, 277–284, 2000.

Stuiver, M., P. J. Reimer, E. Bard, J. W. Beck, G. S. Burr, K. A. Hughen, B. Kromer, F. G. McCormac, J. van der Plicht, and M. Spurk, INTCAL98 radiocarbon age calibration, 24,000-0 cal BP, *Radiocarbon*, *40*, 1041–1083, 1998.

Teller, J. T., North America and adjacent oceans during the last deglaciation, in *The Geology of North America*, edited by W. F. Ruddiman and H. E. Wright, pp. 39–69, Geol. Soc. of Am., Boulder, Col., 1987.

van der Plas, L., and A. C. Tobi, A chart for judging the reliability of point counting results, *Am. J. Sci.*, *263*, 87–90, 1965.

Van Kreveld, S., M. Sarnthein, H. Erlenkeuser, P. Grootes, S. Jung, M. J. Nadeau, U. Pflaumann, and A. Voelker, Potential links between surging ice sheets, circulation changes, and the Dansgaard-Oeschger cycles in the Irminger Sea, 60–18 kyr, *Paleoceanography*, *15*, 425–442, 2000.

Voelker, A., Zur Deutung der Dansgaard Oeschger Ereignisse in ultrahochauflösenden Sedimentprofilen aus dem Europäischen Nordmeer, PhD thesis, 100 pp., Univ. of Kiel, Kiel, 1999.

Voelker, A. H. L., M. Sarnthein, P. Grootes, H. Erlenkeuser, C. Laj, A. Mazaud, M.-J. Nadeau, and M. Schleicher, Correlation of marine ^{14}C ages from the Nordic Seas with the GISP2 isotope record: Implications for ^{14}C calibration beyond 25 ka BP, *Radiocarbon*, *40*, 517–534, 1998.

Voelker, A. H. L., P. M. Grootes, M.-J. Nadeau, and M. Sarnthein, ^{14}C levels in the Iceland Sea from 25–53 kyr and their link to the Earth's magnetic field intensity, *Radiocarbon*, *42*, 437–452, 2000.

Vogelsang, E., M. Sarnthein, and U. Pflaumann, $\delta^{18}O$ Stratigraphy, chronology, and sea surface temperatures of Atlantic sediment records (GLAMAP 2000 Kiel), *Rep. 13*, pp. 1–11, Inst. für Geowiss., Christian-Albrechts Univ. of Kiel, Kiel, 2001.

Waelbroeck, C., L. Labeyrie, J.-C. Duplessy, J. Guiot, M. Labracherie, H. Leclaire, and J. Duprat, Improving past surface temperature estimates based on planktonic fossil faunas, *Paleoceanography*, *13*, 272–282, 1998.

Weinelt, M., M. Sarnthein, H. Schulz, U. Pflaumann, S. Jung, and H. Erlenkeuser, Ice-free Nordic Seas during the Last Glacial Maximum?–Potential sites of deepwater formation, *Paleoclim. Data Model.*, *1*, 283–309, 1996.

Weinelt, M., et al., Paleoceanographic proxies in the northern North Atlantic, in *The Northern North Atlantic: A Changing Environment*, edited by P. Schäfer et al., pp. 319–352, Springer-Verlag, New York, 2001.

Yokoyama, Y., K. Lambeck, P. De Deckker, P. Johnston, and L. K. Fifield, Timing of the Last Glacial Maximum from observed sea-level minima, *Nature*, *406*, 713–716, 2000.

H. Erlenkeuser, Leibniz Labor für Altersbestimmung und Isotopenforschung, Kiel University, Kiel, Germany.

M. Kucera, Department of Geology, Royal Holloway, University of London, Egham, Surrey, TW20 0EX UK. (m.kucera@gl.rhul.ac.uk)

B. A. Malmgren, Department of Earth Sciences-Marine Geology, University of Goteborg, Earth Sciences Center, Box 460, SE-405 30, Goteborg, Sweden. (bjorn.malmgren@marine-geology.gu.se)

U. Pflaumann, M. Sarnthein, E. Vogelsang, and M. Weinelt, Institut fuer Geowissenschaften, Universitaet Kiel, Olshausenstrasse 40, D-24118 Kiel, Germany. (up@gpi.uni-kiel.de; ms@gpi.uni-kiel.de; mw@gpi.uni-kiel.de)

A. Voelker, Instituto Geológico e Mineiro, Departamento de Geologia Marinha, Estrada da Portela, Zambujal, P-2720 Alfragide, Portugal. (antje.voelker@igm.pt)